3D Graphene–Cobalt Oxide Electrode for High-Performance Supercapacitor and Enzymeless Glucose Detection

Xiao-Chen Dong,[†,*] Hang Xu,[†] Xue-Wan Wang,[‡] Yin-Xi Huang,[‡] Mary B. Chan-Park,[‡] Hua Zhang,[§] Lian-Hui Wang,[†] Wei Huang,[†] and Peng Chen[‡,*]

[†]Key Laboratory for Organic Electronics & Information Displays (KLOEID), Institute of Advanced Materials (IAM), Nanjing University of Posts and Telecommunications (NUPT), 9 Wenyuan Road, Nanjing, 210046, China, [‡]School of Chemical and Biomedical Engineering, Nanyang Technological University, Singapore 637457, and [§]School of Materials Science and Engineering, Nanyang Technological University, Singapore 639798

ABSTRACT

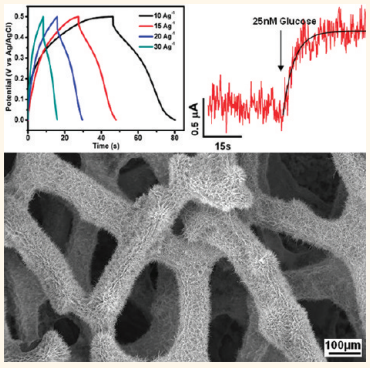

Using a simple hydrothermal procedure, cobalt oxide (Co_3O_4) nanowires were *in situ* synthesized on three-dimensional (3D) graphene foam grown by chemical vapor deposition. The structure and morphology of the resulting 3D graphene/Co_3O_4 composites were characterized by scanning electron microscopy, transmission electron microscopy, X-ray diffraction, and Raman spectroscopy. The 3D graphene/Co_3O_4 composite was used as the monolithic free-standing electrode for supercapacitor application and for enzymeless electrochemical detection of glucose. We demonstrate that it is capable of delivering high specific capacitance of ~1100 F g^{-1} at a current density of 10 A g^{-1} with excellent cycling stability, and it can detect glucose with a ultrahigh sensitivity of 3.39 mA mM^{-1} cm^{-2} and a remarkable lower detection limit of <25 nM (S/N = 8.5).

KEYWORDS: 3D graphene · cobalt oxide · supercapacitor · enzymeless detection

Graphene, a two-dimensional monolayer of sp^2-hybridized carbon atoms, has attracted enormous interest in recent years due to its extraordinary electrical properties, unusual mechanical strength, and ultralarge specific surface area.[1−3] It is providing tremendous new advances in various fields, such as field-effect transistors,[4−6] biological/chemical sensors,[7−10] energy storage[11−13] and conversion[14] devices, and transparent conductors.[15−17] In addition, compositing graphene with other functional nanomaterials to attain synergistic effects leads to vast unprecedented possibilities.[18−22]

In particular, many approaches have been explored to fabricate graphene-based nanocomposites for high-performance supercapacitors and biosensors.[23−27] In current developments, chemically reduced graphene oxide (rGO) is used as the substitute for pristine graphene because of the low-cost large-scale production enabled by the chemical exfoliation processes.[28] However, the exceptional properties of graphene are severely impaired in rGO due to abundant defects and chemical moieties created in the synthesis procedures. In graphene composites, aggregation and stacking between individual graphene sheets driven by the strong $\pi-\pi$ interaction greatly compromise the intrinsic high specific surface area of graphene. Furthermore, the high conductivity of graphene is also largely compromised due to intersheet contact resistance. The recently demonstrated chemical vapor deposition (CVD)-grown graphene foams[29−31] promise to alleviate the aforementioned problems that currently plague the performance of graphene composites. The three-dimensional (3D) graphene foams are seamlessly continuous and a highly conductive graphene network that is free of defects and intersheet junctions. Their 3D porous structure is ideal to serve as the scaffold for fabrication of monolithic composite electrodes.

Cobaltosic oxide (Co_3O_4) is a transition metal oxide with intriguing electronic, optical, electrochemical, and electrocatalytic properties. Co_3O_4-based nanocomposites have demonstrated great potentials in the applications of supercapacitors,[32] heterogeneous catalysts,[33] electrochemical sensors,[34] and Li-ion rechargeable batteries.[35] In the

* Address correspondence to iamxcdong@njupt.edu.cn, chenpeng@ntu.edu.sg.

Received for review January 9, 2012 and accepted March 21, 2012.

Published online March 21, 2012
10.1021/nn300097q

© 2012 American Chemical Society

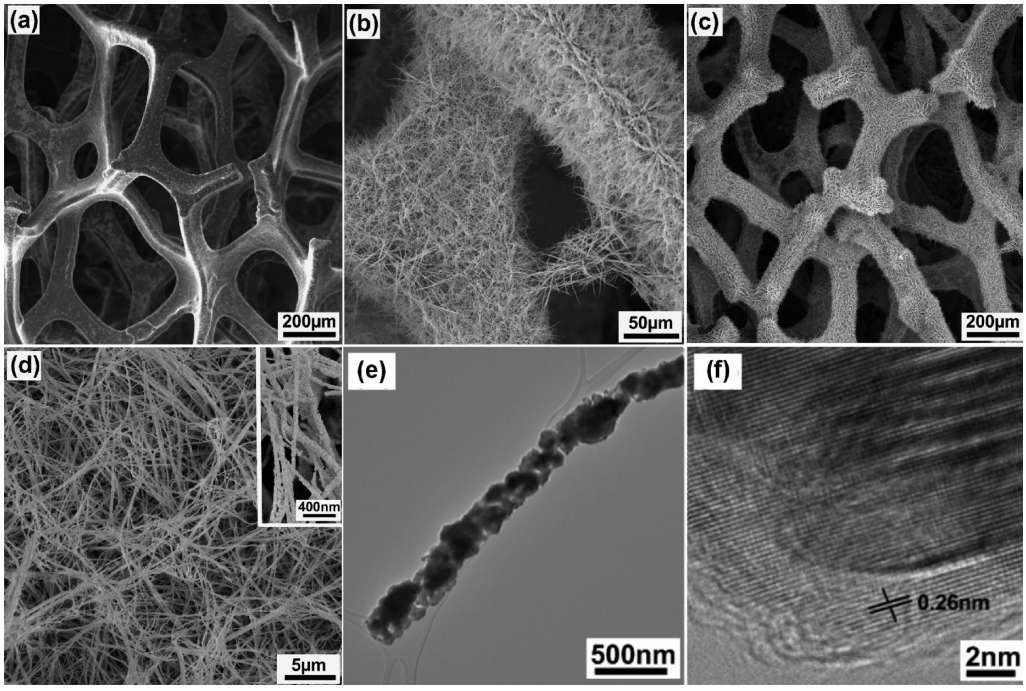

Figure 1. SEM images of (a) 3D graphene foam, (b) 3D graphene/Co_3O_4 nanowire composite. (c,d) Low- and high-magnification SEM images of graphene/Co_3O_4 nanowire composite. Inset panel d shows an enlarged view. (e,f) Low- and high-resolution TEM images of Co_3O_4 nanowire grown on the surface of 3D graphene foam.

present study, we synthesize a 3D graphene/Co_3O_4 nanowire composite. Serving as a free-standing monolithic electrode, it demonstrates remarkable performance in supercapacitor application and in enzyme-free electrochemical detection of glucose.

RESULTS AND DISCUSSION

The morphology and structure of the graphene foam and graphene/Co_3O_4 composites were examined by SEM and TEM, as shown in Figure 1. The graphene foam is a 3D porous structure with a smooth and thin graphene skeleton (Figure 1a). The width of the graphene skeleton is about 100−120 μm. For the graphene/Co_3O_4 composite, the graphene skeleton is fully and uniformly covered by the network of Co_3O_4 nanowires (Figure 1b−d). The thickness of the Co_3O_4 nanowire shell is about 10 μm according to the increase in the width of the graphene skeleton. The high-magnification SEM image reveals that the Co_3O_4 nanowires are about 200−300 nm in diameter and several micrometers in length (Figure 1d), and as shown in the TEM image (Figure 1e), the Co_3O_4 nanowires are composed of numerous nanoparticles. The 3D structrure of graphene foam, the nanoporous mesh of Co_3O_4 nanowires, and the rough surface of individual nanowires together provide a large accessible surface area. The high-resolution TEM image shows that the Co_3O_4 nanowires exhibit high crystallinity with a lattice spacing of 0.26 nm corresponding to the interspacing of the (311) planes.

Figure 2a shows the XRD patterns of 3D graphene and the graphene/Co_3O_4 nanowire composite. The 3D graphene shows two significant diffraction peaks at 2θ = 26.5 and 54.6° attributed to the (002) and (004) reflections of graphitic carbon, respectively (JCPDS 75-1621). In addition to the characteristic peaks from graphene, the graphene/Co_3O_4 nanowire composite presents nine obvious diffraction peaks. They conincide with the (111), (220), (311), (222), (400), (422), (511), (440), and (531) planes in the standard Co_3O_4 spectrum (JCPDS 42-1467). Figure 2b shows the Raman spectra of graphene foam and the graphene/Co_3O_4 composite. Except for the characteristic G and 2D peaks at ~1575 and 2740 cm^{-1} from graphene,[36] four characteristic peaks from the cobaltosic oxides at 464, 507, 606, and 675 cm^{-1} (corresponding to E_g, F_{2g}^1, F_{2g}^2, and A_g^1 modes of the crystalline Co_3O_4, respectively)[37] are identified in the spectrum of the composite. Both XRD and Raman measurments confirm the successful integration of 3D graphene foam and Co_3O_4 nanowires. In addition, there is no obvious graphene D band at ~1350 cm^{-1}, indicating that the graphene foam is of high quality, that is, lack of defects.[38] The integral ratio of the 2D and G band indicates that the as-grown graphene foams consist of mainly one- to few-layered domains.[29]

Graphene material/metal oxide composites with surface-anchored, wrapped, encapsulated, sandwiched, layer-by-layer assembled, and randomly mixed architeture have recently been utilized as advanced electrode materials for supercapacitors.[39] They have demonstrated

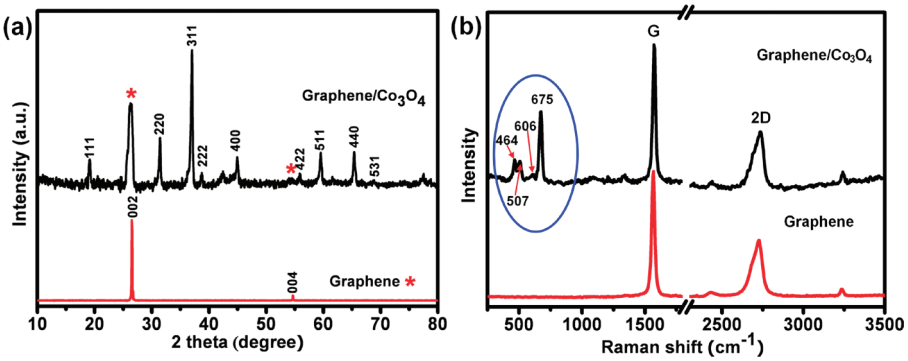

Figure 2. (a) XRD patterns and (b) Raman spectra of graphene and the graphene/Co_3O_4 nanowire composite.

significant improvement in electrochemical properties as compared with the individual constituents. Here, we first sought to investigate the electrochemical performance of 3D graphene/Co_3O_4 composite toward supercapacitor application. Owing to the excellent mechanical strength of graphene, the graphene/Co_3O_4 composite is able to serve as a free-standing monolithic electrode despite its lightness (80 mg/cm^3).

Figure 3a presents the cyclic voltammetry (CV) curves over a voltage range from 0 to 0.5 V for the 3D graphene and graphene/Co_3O_4 composite electrodes measured at a scan rate of 50 mV/s. Evidently, the area surrounded by the CV curve is dramatically enhanced by the introduction of Co_3O_4 nanowires onto 3D graphene foam. These results indicate a large specific capacitance associated with the composite electrode and suggest that it is originiated from the pseudocapacitance of the electrochemically active Co_3O_4 nanowires instead of double-layer capacitance from the graphene foam. Increasing the scan rate leads to further augment of the CV curve and the redox peaks (Figure 3b), indicating that the redox reactions of Co_3O_4 are rapid. Figure 3c depicts the charge−discharge behavior of the graphene/Co_3O_4 composite electrode between 0 and 0.5 V at different current densities. The specific capacitance can be caculated as follows.[40] $C_m = It/\Delta Vm$, where C_m is the specific capacitance of the electrode (F g^{-1}), I is the charge/discharge current (A), t is the discharge time (s), ΔV is the potential window, and m is the mass of the graphene/Co_3O_4 composite electrode. The specific capacitance of the graphene/Co_3O_4 composite electrode is calculated to be about 768, 618, 552, and 456 F/g at the current densities of 10, 15, 20, and 30 A/g, respectively.

The cycling stability of the graphene/Co_3O_4 electrode was examined over a large number of charge−discharge cycles at the current density of 10 A g^{-1}, as shown in Figure 3d. Interestingly, the specific capacitance of the composite electrode can be further enhanced to ~1100 F/g after 500 cycles and stays stable afterward. Such an activation process may result from the more complete intercalation and deintercalation of electrochemical species after some initial cycles.[41] The electrochemical stability of the composite electrode is also evidenced in Figure 3e, which shows that even after a long period of charge−discharge (>25000 s), the charge−discharge curves remain undistorted and essentially symmetric. Taken together, our results demonstrate that the 3D graphene/Co_3O_4 composite electrode gives a large specific capacitance and excellent cycling stability, promising for the development of high-performance supercapactiors. This specific capacitance of our 3D graphene/Co_3O_4 electrode is several times larger than that of the previously reported reduced graphene oxide/Co_3O_4 composite electrodes.[42,43] It is also much larger than that of many previously reported graphene-based composite electrodes, such as graphene/MnO_2,[44] graphene/NiO,[45] or graphene/PANI[46] electrodes.

Electrochemical impedance spectroscopy (EIS) was also employed to characterize the 3D graphene and composite electrode. As shown in the Nyquist plots (Figure 3f), the equivalent series resistance (ESR) of the graphene/Co_3O_4 composite electrode (3.0 Ω) is much smaller than that of the bare graphene foam electrode (9.0 Ω), indicating a lower diffusion resistance and charge-transfer resistance. This further suggests that the 3D graphene/Co_3O_4 electrode is advantageous for electrochemical applications, such as electrochemical sensing. Co_3O_4 is electrocatalytically active. Recently, Ding *et al.* demonstrated the use of electrospun Co_3O_4 nanofibers for sensitive, selective, and non-enzymatic detection of glucose.[47] Prompted by this work, we sought to study the ability of the 3D graphene/Co_3O_4 electrode in non-enzymatic detection of glucose.

Detecting glucose is of paramount importance to the diagnosis and management of diabetes. For most glucose sensors, the detection is indirect, relying on enzymes, for example, glucose oxidase. The need for enzyme proteins complicates the sensor construction, increases the cost, and compromises the sensitivity, stability, and reproducibility of the sensor due to the poor tolerance to nonphysiological chemical environments and the sensitivity to temperature, pH, humidity, *etc*. Several studies have shown that Co_3O_4 nanostructures are capable of catalyzing glucose oxidation and

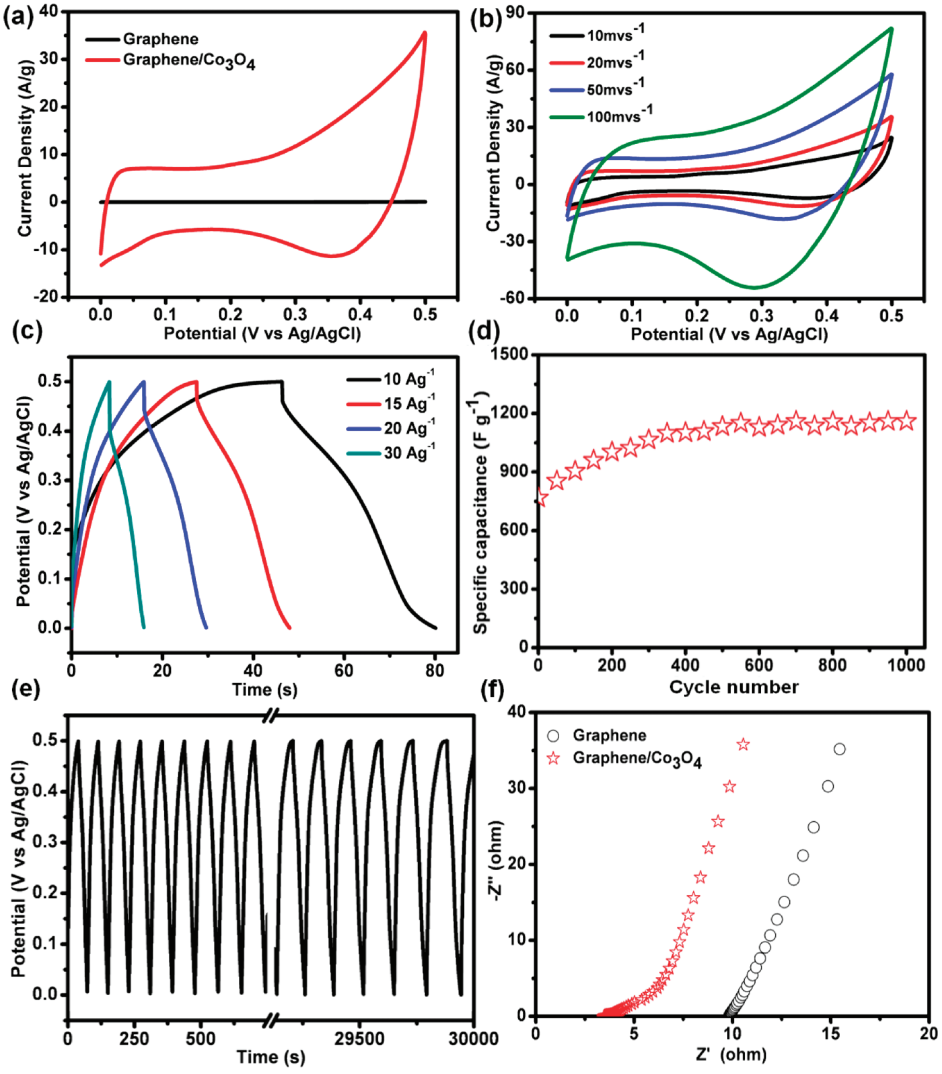

Figure 3. Electrochemical performance of the 3D graphene electrodes measured in 2.0 M KOH solution. (a) CV curves of 3D graphene and graphene/Co_3O_4 composite electrodes measured at a scan rate of 50 mV/s. (b) CV curves of 3D graphene/Co_3O_4 composite electrode at scan rates of 5, 10, 20, and 50 mV s^{-1}. (c) Galvanostatic charge/discharge curves of graphene/Co_3O_4 composite electrode at different current densities. (d) Cycling performance of graphene/Co_3O_4 composite electrode at a current density of 10.0 A g^{-1}. (e) Charge/discharge profile of the composite electrode at a current density of 10.0 A g^{-1}. (f) Nyquist plots of 3D graphene and graphene/Co_3O_4 composite electrodes.

therefore enable direct electrochemical detection of glucose without the need of any enzymes or other mediators.[47,48]

As previously demonstrated, glucose detection is optimized in low-strength alkaline solutions.[47] To benchmark with Ding's work, we also used 0.1 M NaOH as the electrolyte. Figure 4a shows the CV curves of the graphene/Co_3O_4 composite electrode at different scan rates. In agreement with Ding's report,[47] two pairs of redox peaks (I/II and III/IV) are observed, resulting from the reversible transition between Co_3O_4 and CoOOH (I/II) and transition between CoOOH and CoO_2 (III/IV). The reactions can be formulated as $Co_3O_4 + OH^- + H_2O \leftrightarrow 3CoOOH + e^-$ and $CoOOH + OH^- \leftrightarrow CoO_2 + H_2O + e^-$.[49] With an increase of the scan rate, both of the redox current peaks increase, suggesting a surface-controlled electrochemical process. As shown in Figure 4b, introduction of glucose causes obvious increase of the oxidation current at peak III (at ~0.58 V) in a concentration-dependent manner while the current at peak I (at ~0.25 V) remains nearly constant. As elegantly explained by Ding *et al.*, this is due to glucose oxidation to gluconolactone catalyzed by conversion of CoO_2 to CoOOH (redox pair III/IV): $2CoO_2 + C_6H_{12}O_6$ (glucose) $\rightarrow 2CoOOH + C_6H_{10}O_6$. Holding at the oxidation potential of peak III (+0.58 V), the amperometric responses of the graphene/Co_3O_4 composite electrode to successive addition of glucose to *increasing* concentrations were measured (Figure 4c). The dose response curve (amperometric current increase *vs* glucose concentration) is plotted in Figure 4d. An extraordinary sensitivity of 3.39 mA mM^{-1} cm^{-2} is obtained in the linear response range (up to 80 μM). Such sensitivity predicts a remarkable sub-100 nM

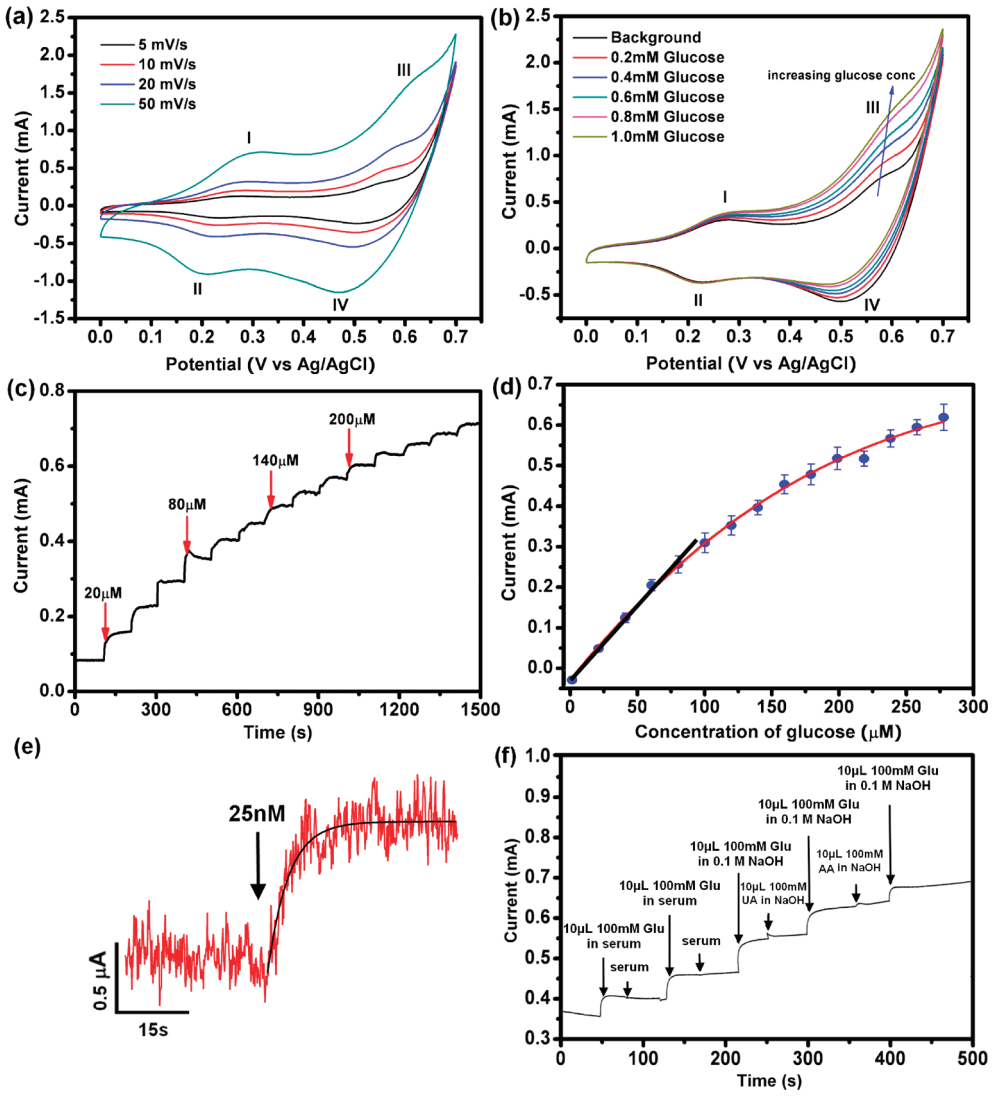

Figure 4. Detection of glucose in 0.1 M NaOH solution using the 3D graphene/Co_3O_4 composite electrode. (a) CV curves measured at different scan rates (5, 10, 20, and 50 mV/s). (b) CV curves in the presence of various concentrations of glucose (0, 0.2, 0.4, 0.6, 0.8, and 1 mM), at the scan rate of 20 mV/s. (c) Amperometric response of the composite electrode (holding at 0.58 V) upon addition of glucose to increasing concentrations. (d) Average dose response curve (amperometric current response *vs* glucose concentration) obtained from three different sensors, with a linear fitting at lower concentration range and an exponential fitting at higher concentration range. The error bars indicate the standard deviations. (e) Amperometric response to 25 nM glucose. An exponential fitting with a time constant of ~3.7 s is shown. (f) Amperometic response to the addition of 10 μL of different analytes to 20 mL of electrolyte (0.1 M NaOH). AA = ascorbic acid; UA = uric acid. The serum sample is made of 100 μg/mL of fetal bovine serum in Dulbecco's modified Eagle medium (DMEM).

lower detection limit (LOD). Indeed, as shown in Figure 4e, obvious amperometric response can be triggered by the addition of glucose to an equilibrium concentration of 25 nM, with a signal-to-noise ratio (S/N) of ~8.5. This detection limit is more than an order lower than the extrapolated LOD of the Co_3O_4 nanofiber electrode devised by Ding *et al.* (970 nM with S/N = 3).[47] The sensitivity and LOD of our 3D graphene/Co_3O_4 electrode are also significantly superior than the previously reported graphene-based electrochemical and electrical sensors assisted by enzymes.[50,51]

In a comparative control experiment (Figure S1 in the Supporting Information), Co_3O_4 nanowires were synthesized using the same hydrothermal process and coated on glassy carbon electrodes. In comparison with the 3D graphene/Co_3O_4 electrode, the CV profile of the planar Co_3O_4 electrode is much narrower, indicating a smaller electrochemical capacitance, and the planar Co_3O_4 electrode's response to glucose is much less sensitive and much slower. This experiment clearly suggests the importance of the 3D graphene support. Furthermore, as shown in Figure 4f, the 3D graphene/Co_3O_4 electrode is insensitive to uric acid and ascorbic acid (biomolecules in blood) and insensitive to the glucose-free serum sample which contains abundant and a large variety of proteins and other molecules. On the other hand, our sensor is sensitive to the serum sample supplemented with glucose. This

experiment indicates the high selectivity of our sensor and its potential for practical use.

CONCLUSIONS

In this study, we demonstrate a facile two-step synthesis route (CVD growth of graphene foam and *in situ* hydrothermal synthesis of Co_3O_4 nanowires) to produce a 3D graphene/Co_3O_4 composite. Co_3O_4 nanowires with uniform diameter and high crystallinity form a dense naonmesh covering the 3D graphene skeleton. Due to the superior mechanical strength of graphene, the 3D graphene/Co_3O_4 composite can work as a free-standing electrode despite its lightness, and such a monolithic 3D electrode demonstrates remarkable performance as a supercapacitor and for enzyme-free ultrasensitive detection of glucose because of the synergistic integration of the two novel nanomaterials. First, the three-dimensionally multiplexed and highly conductive pathways provided by the defect-free graphene foam ensure rapid charge transfer and conduction. In addition, Co_3O_4 nanowires exhibit exceptional electrochemical and electrocatalytic properties. Lastly, the 3D graphene/Co_3O_4 electrode provides an enormous accessible active area. The bare graphene foam has a high specific surface area of $\sim$850 $m^2\,g^{-1}$,[29] and this is further increased greatly by the Co_3O_4 nanomesh surrounding the graphene scaffold. Also, the open pore system of the composite is beneficial to ion diffusion and transport kinetics.

As demonstrated here, graphene foam is uniquely advantageous to serve as a 3D support of large capacity to uniformly anchor metal oxides with well-defined size, shapes, and crystallinity. Agglomeration, the common phenomenon of metallic oxide preparations, is no longer an issue. The multifunctionalities and improved performance that come from the synergistic cooperation between graphene and metal oxides promise many novel applications.

MATERIALS AND METHODS

Synthesis of 3D Graphene Foam. Similar to that previously reported,[29] 3D graphene was synthesized by chemical vapor deposition (CVD) using nickel foam as the substrate, except that ethanol was used as the carbon source for graphene growth under atmospheric pressure.[52,53] The nickel foam (0.5 mm thick, Alantum Advanced Technology Materials, China) placed into a quartz tube was heated to 1000 °C at a 50 °C/min heating rate and maintained for 10 min under atmospheric pressure with a gas flow of H_2/Ar (H_2/Ar = 25:50 sccm) to clean the surface of nickel foam. After 20 min of growth, the sample is rapidly cooled to the room temperature at a cooling rate of 100 °C/min under H_2/Ar flow. Finally, the sample was cut into small pieces (1 cm × 1 cm), and the nickel substrate was etched away with HCl (3 M) solution at 80 °C to leave the free-standing 3D graphene foams.

Preparation of Graphene/Co_3O_4 Nanowire Composite. $CoCl_2 \cdot 6H_2O$ (1 mmol) (Sigma-Aldrich USA) and urea (1.0 mmol) (Sigma-Aldrich USA) were added to 20 mL of water and stirred for 10 min. The mixture was then transferred to a Teflon-lined stainless steel autoclave of 30 mL capacity. Subsequently, the 3D graphene foams fixed on a glass slide were immersed into the solution. This was followed by autoclaving at 120 °C for 16 h. After cooling to room temperature, the graphene foams with light-pink deposits were washed with deionized water and dried at 50 °C. Finally, the sample was heated at 450 °C for 2 h.

Characterization. Raman spectra were recorded at ambient temperature on a WITeck CRM200 confocal microscopy Raman system with 488 nm wavelength laser. The X-ray diffraction (XRD) was carried out on a Bruker D8 Avance diffractometer using Cu Kα radiation. The morphology of the composite was examined by field-emission scanning electron microscopy (FESEM, JSM-6700F, JEOL). Transmission electron microscopy (TEM) was conducted with a JEOL JEM-1400F microscope operated at 200 KV.

Electrochemical Measurement. Cyclic voltammetry (CV), electrochemical impedance spectroscopy (EIS), and amperometry measurements were performed using a CHI660D electrochemical workstation (Chenhua, Shanghai). The 3D graphene/Co_3O_4 composite serves as the working electrode, while a platinum foil electrode and a Ag/AgCl electrode were used as the counter and reference electrodes, respectively. EIS measurements were conducted in the frequency range from 0.01 to 100 kHz at open-circuit potential with an ac perturbation of 5.0 mV.

Conflict of Interest: The authors declare no competing financial interest.

Acknowledgment. We acknowledge the financial support from NNSF of China (50902071, 61076067, BZ2010043), the National Basic Research Program of China (2009CB930601, 2012CB933301), the Ministry of Education of China (IRT1148), A Project Funded by the Priority Academic Program Development of Jiangsu Higher Education Institutions, CRP grant from National Research Foundation of Singapore (NRF-CRP-07-2), and AcRF Tier 2 grants of Ministry of Education of Singapore (MOE2010-T2-1-060, MOE2011-T2-2-010).

Supporting Information Available: Additional information on CV plots of Co_3O_4 nanowire modified glassy carbon electrode and the amperometric response to glucose are provided. This material is available free of charge *via* the Internet at http://pubs.acs.org.

REFERENCES AND NOTES

1. Geim, A. K.; Novoselov, K. S. The Rise of Graphene. *Nat. Mater.* **2007**, *6*, 183–191.
2. Eda, G.; Chhowalla, M. Chemically Derived Graphene Oxide: Towards Large-Area Thin-Film Electronics and Optoelectronics. *Adv. Mater.* **2010**, *22*, 2392–2415.
3. Zhu, Y. W.; Murali, S.; Cai, W. W.; Li, X. S.; Suk, J. W.; Potts, J. R.; Ruoff, R. S. Graphene and Graphene Oxide: Synthesis, Properties, and Applications. *Adv. Mater.* **2010**, *22*, 3906–3924.
4. Xu, H.; Zhang, Z.; Wang, Z. X.; Wang, S.; Liang, X.; Peng, L. M. Quantum Capacitance Limited Vertical Scaling of Graphene Field-Effect Transistor. *ACS Nano* **2011**, *5*, 2340–2347.
5. Schwierz, F. Graphene Transistors. *Nat. Nanotechnol.* **2010**, *5*, 487–496.
6. Novoselov, K. S.; Geim, A. K.; Morozov, S. V.; Jiang, D.; Zhang, Y.; Dubonos, S. V.; Grigorieva, I. V.; Firsov, A. A. Electric Field Effect in Atomically Thin Carbon Films. *Science* **2004**, *306*, 666–669.
7. Huang, Y. X.; Dong, X. C.; Liu, Y. X.; Li, L. J.; Chen, P. Graphene-Based Biosensors for Detection of Bacteria and Their Metabolic Activities. *J. Mater. Chem.* **2011**, *21*, 12358–12362.
8. Fowler, J. D.; Alle, M. J.; Tung, V. C.; Yang, Y.; Kaner, R. B.; Weiller, B. H. Practical Chemical Sensors from Chemically Derived Graphene. *ACS Nano* **2009**, *3*, 301–306.

9. Dong, X. C.; Shi, Y. M.; Huang, W.; Chen, P.; Li, L. J. Electrical Detection of DNA Hybridization with Single-Base Specific Using Transistors Based on CVD-Grown Graphene Sheets. *Adv. Mater.* **2010**, *22*, 1649–1653.
10. Liu, Y. X.; Dong, X. C.; Chen, P. Biological and Chemical Sensors Based on Graphene Materials. *Chem. Soc. Rev.* **2012**, *41*, 2283–2307.
11. Wu, Q.; Xu, Y. X.; Yao, Z. Y.; Liu, A. R.; Shi, G. Q. Supercapacitors Based on Flexible Graphene/Polyaniline Nanofiber Composite Films. *ACS Nano* **2010**, *4*, 1963–1970.
12. Zhu, Y. W.; Murali, S.; Stoller, M. D.; Ganesh, K. J.; Cai, W.; Ferreira, P.; Pirkle, A.; Wallace, R.; Cychosz, K.; Thommes, M.; *et al.* Carbon-Based Supercapacitors Produced by Activation of Graphene. *Science* **2011**, *332*, 1537–1541.
13. Yoo, E.; Zhou, H. S. Li-Air Rechargeable Battery Based on Metal-Free Graphene Nanosheet Catalysts. *ACS Nano* **2011**, *5*, 3020–3026.
14. Yu, D.; Park, K.; Durstock, M.; Dai, L. M. Fullerence-Grafted Graphene for Efficient Bulk Heterojunction Polymer Photovoltaic Devices. *J. Phys. Chem. Lett.* **2011**, *2*, 1113–1118.
15. Bae, S.; Kim, H.; Lee, Y.; Xu, X. F.; Park, J. S.; Zheng, Y.; Balakrishnan, J.; Lei, T.; Kim, H. R.; Song, Y., Il.; *et al.* Roll-to-Roll Production of 30-in. Graphene Films for Transparent Electrodes. *Nat. Nanotechnol.* **2010**, *5*, 574–578.
16. Kim, K. S.; Zhao, Y.; Jang, H.; Lee, S. Y.; Kim, J. M.; Kim, K. S.; Ahn, J.; Kim, P.; Choi, J.; Hong, B. H. Large-Scale Pattern Growth of Graphene Films for Stretchable Transparent Electrodes. *Nature* **2009**, *457*, 706–710.
17. Kasry, A.; Kuroda, M. A.; Martyna, G. J.; Tulevski, G. S.; Bol, A. A. Chemical Doping of Large-Area Stacked Graphene Films for Use as Transparent, Conducting Electrodes. *ACS Nano* **2010**, *4*, 3839–3844.
18. Tung, V. C.; Huang, J.; Tevis, L.; Kim, F.; Kim, J.; Chu, C.; Stupp, S. I.; Huang, J. X. Surfactant-Free Water-Processable Photoconductive All-Carbon Composite. *J. Am. Chem. Soc.* **2011**, *133*, 4940–4947.
19. Wang, S.; Tambraparni, M.; Qiu, J.; Tipton, J.; Dean, D. Thermal Expansion of Graphene Composites. *Macromolecules* **2009**, *42*, 5251–5255.
20. Chandra, V.; Park, J.; Chun, Y.; Lee, J. W.; Hwang, I.; Kim, K. S. Water-Dispersible Magnetite-Reduced Graphene Oxide Composites for Arsenic Removal. *ACS Nano* **2010**, *4*, 3979–6986.
21. Mukherji, A.; Seger, B.; Lu, G. Q.; Wang, L. Z. Nitrogen Doped $Sr_2Ta_2O_7$ Coupled with Graphene Sheets as Photocatalysts for Increased Photocatalytic Hydrogen Production. *ACS Nano* **2011**, *5*, 3483–3492.
22. Huang, X.; Qi, X. Y.; Zhang, H. Graphene-Based Composites. *Chem. Soc. Rev.* **2012**, *41*, 666–686.
23. Yan, J.; Fan, Z. J.; Wei, T.; Qian, W. Z.; Zhang, M. L.; Wei, F. Fast and Reversible Surface Redox Reaction of Graphene–MnO_2 Composites as Supercapacitor Electrodes. *Carbon* **2010**, *48*, 3825–3833.
24. Guo, S. J.; Dong, S. J. Graphene Nanosheet: Synthesis, Molecular Engineering, Thin Film, Hybrids, and Energy and Analytical Applications. *Chem. Soc. Rev.* **2011**, *40*, 2644–2672.
25. Dong, X. C.; Huang, W.; Chen, P. *In-Situ* Synthesis of Reduced Graphene Oxide and Gold Nano-composites for Nanoelectronics and Biosensing. *Nanoscale Res. Lett.* **2011**, *6*, 60.
26. Davies, A.; Audette, P.; Farrow, B.; Hassan, F.; Chen, Z. W.; Choi, J. Y.; Yu, A. P. Graphene-Based Flexible Supercapacitors: Pulse-Electropolymerization of Polypyrrole on Free-Standing Graphene Films. *J. Phys. Chem. C* **2011**, *115*, 17612–17620.
27. Sudibya, H. G.; He, Q; Zhang, H; Chen, P. Electrical Detection of Metal Ions Using Field-Effect Transistors Based on Micropatterned Reduced Graphene Oxide Films. *ACS Nano* **2011**, *5*, 1990–1994.
28. Dong, X. C.; Su, C. Y.; Zhang, W. J.; Zhao, J. W.; Ling, Q. D.; Huang, W.; Chen, P.; Li, L. J. Ultra-large Single-Layer Graphene Obtained from Solution Chemical Reduction and Its Electrical Properties. *Phys. Chem. Chem. Phys.* **2010**, *12*, 2164–2169.
29. Chen, Z.; Ren, W.; Gao, L.; Liu, B.; Pei, S.; Cheng, H. M. Three-Dimensional Flexible and Conductive Interconnected Graphene Networks Grown by Chemical Vapor Deposition. *Nat. Mater.* **2011**, *10*, 424–428.
30. Cao, X. H.; Shi, Y. M.; Shi, W. H.; Lu, G.; Huang, X.; Yan, Q. Y.; Zhang, Q. C.; Zhang, H. Preparation of Novel 3D Graphene Networks for Supercapacitor Applications. *Small* **2011**, *7*, 3163–3168.
31. Yong, Y. C.; Dong, X. C.; Chan-Park, M. B.; Song, H.; Chen, P. Macroporous and Monolithic Anode Based on Polyaniline Hybridized Three-Dimensional Graphene for High-Performance Microbial Fuel Cells. *ACS Nano* **2012**, 10.1021/nn204656d.
32. Xia, X. H.; Tu, J. P.; Wang, X. L.; Gu, C. D.; Zhao, X. B. Mesoporous Co_3O_4 Monolayer Hollow-Shape Array as Electrochemical Pseudocapacitor Materials. *Chem. Commun.* **2011**, *47*, 5786–5788.
33. Liang, Y.; Li, Y.; Wang, H.; Zhou, J.; Wang, J.; Regier, T.; Dai, H. J. Co_3O_4 Nanocrystals on Graphene as a Synergistic Catalyst for Oxygen reduction Reaction. *Nat. Mater.* **2011**, *10*, 780–786.
34. Kuang, C.; Lin, C.; Lai, Y.; Vittal, R.; Ho, K. C. Cobalt Oxide Acicular Nanorods with High Sensitivity for the Non-enzymatic Detection of Glucose. *Biosens. Bioelectron.* **2011**, *27*, 125–131.
35. Poizot, P.; Laruelle, S.; Grugeon, S.; Dupont, L.; Tarascon, J. M. Nano-Sized Transition-Metal Oxides as Negative-Electrode Materials for Lithium-Ion Battery. *Nature* **2000**, *407*, 496–499.
36. Dong, X. C.; Shi, Y. M.; Zhao, Y.; Chen, D. M.; Ye, J.; Yao, Y. G.; Gao, F.; Ni, Z. H.; Yu, T.; Shen, Z. X.; *et al.* Symmetry Breaking of Graphene Monolayers by Molecular Decoration. *Phys. Rev. Lett.* **2009**, *102*, 135501.
37. Wang, G. X.; Shen, X. P.; Horvat, J.; Wang, B.; Liu, H.; Wexler, D.; Yao, J. Hydrothermal Synthesis and Optical, Magnetic, and Supercapacitance Properties of Nanoporous Cobalt Oxide Nanorods. *J. Phys. Chem. C* **2009**, *113*, 4357–4361.
38. Dong, X. C.; Fu, D. L.; Fang, W. J.; Shi, Y. M.; Chen, P.; Li, L. J. Doping Single-Layer Graphene with Aromatic Molecules. *Small* **2009**, *5*, 1422–1426.
39. Wu, Z. S.; Zhou, G.; Yin, L.; Ren, W.; Li, F.; Cheng, H. M. Graphene/Metal Oxide Composite Electrode Materials for Energy Storage. *Nano Energy* **2012**, *1*, 107–131.
40. Liu, C. G.; Yu, Z.; Neff, D.; Zhamu, A.; Jang, B. Z. Graphene-Based Supercapacitor with an Ultrahigh Energy Density. *Nano Lett.* **2010**, *10*, 4863–4868.
41. Lu, X.; Zheng, D.; Zhai, T.; Liu, Z.; Huang, Y.; Xie, S.; Tong, Y. Facile Synthesis of Large-Area Manganese Oxide Nanorod Arrays as a High-Performance Electrochemical Supercapacitor. *Energy Environ. Sci.* **2011**, *4*, 2915–2921.
42. Yan, J.; Wei, T.; Qiao, W.; Shao, B.; Zhao, Q.; Zhang, L.; Fan, Z. Rapid Microwave-Assisted Synthesis of Graphene Nanosheet/Co_3O_4 Composite for Supercapacitors. *Electrochim. Acta* **2010**, *55*, 6973–6978.
43. Wang, H. W.; Hu, Z. A.; Chang, Y. Q.; Chen, Y. L.; Zhang, Z. Y. Preparation of Reduced Graphene Oxide/Cobalt Oxide Composites and Their Enhanced Capacitive Behaviors by Homogeneous Incorporation of Reduced Graphene Oxide Sheets in Cobalt Oxide Matrix. *Mater. Chem. Phys.* **2011**, *130*, 672–679.
44. Chen, S.; Zhu, J. W.; Wu, X. D.; Han, Q. F.; Wang, X. Graphene Oxide–MnO_2 Nanocomposites for Supercapacitors. *ACS Nano* **2010**, *4*, 2822–2830.
45. Wu, M. S.; Lin, Y. P.; Lin, C. H.; Lee, J. T. Formation of Nanoscaled Crevices and Spaces in NiO-Attached Graphene Oxide Nanosheets for Supercapacitors. *J. Mater. Chem.* **2012**, *22*, 2442–2448.
46. Wu, Q.; Xu, Y. X.; Yao, Z. Y.; Liu, A. R.; Shi, G. Q. Supercapacitors Based on Flexible Graphene/Polyaniline Nanofiber Composite film. *ACS Nano* **2010**, *4*, 1963–1970.
47. Ding, Y.; Wang, Y.; Su, L.; Bellagamba, M.; Zhang, H.; Lei, Y. Electrospun Co_3O_4 Nanofibers for Sensitive and Selective Glucose Detection. *Biosens. Bioelectron.* **2010**, *26*, 542–548.

48. Yang, J.; Zhang, W. D.; Gunasekaran, S. A Low-Potential, H_2O_2-Assisted Electrodeposition of Cobalt Oxide/Hydroxide Nanostructures onto Vertically-Aligned Multiwalled Carbon Nanotube Arrays for Glucose Sensing. *Electrochim. Acta* **2011**, *16*, 5538–5544.
49. Casella, I. G.; Gatta, M. Study on the Electrochemical Deposition and Properties of Cobalt Oxide Species in Citrate Alkaline Solution. *J. Electroanal. Chem.* **2002**, *534*, 31–38.
50. Kang, X. H.; Wang, J.; Wu, H.; Aksay, I. A.; Liu, J.; Lin, Y. H. Glucose Oxidase-Graphene-Chitosan Modified Electrode for Direct Electrochemistry and Glucose Sensing. *Biosens. Bioelectron.* **2009**, *25*, 901–905.
51. Huang, Y. X.; Dong, X. C.; Shi, Y. M.; Li, C. M.; Li, L. J.; Chen, P. Nanoelectronic Biosensors Based on CVD Grown Graphene. *Nanoscale* **2010**, *2*, 1485–1488.
52. Dong, X. C.; Li, B.; Wei, A.; Cao, X. H.; Park, M.; Zhang, H.; Li, L. J.; Huang, W.; Chen, P. One-Step Growth of Graphene—Carbon Nanotube Hybrid Materials by Chemical Vapor Deposition. *Carbon* **2011**, *49*, 2944–2949.
53. Dong, X. C.; Wang, P.; Fang, W. J.; Su, C. Y.; Chen, Y. H.; Li, L. J.; Huang, W.; Chen, P. Growth of Large-Sized Graphene Thin-Film by Liquid Precursor-Based Chemical Vapor Deposition under Atmospheric Pressure. *Carbon* **2011**, *49*, 3672–3678.